Isotope Dependent System Matrices for High Resolution PET Imaging

Fotis A. Kotasidis, *Member IEEE,* Georgios I. Angelis, *Member IEEE*, Jose Anton-Rodriguez, Julian C. Matthews, *Member IEEE*, Andrew J. Reader, *Member IEEE,* Michael Green, Habib Zaidi, *Senior Member, IEEE*

Abstract— **Measuring and incorporating scanner specific point spread functions (PSFs) within image reconstruction has been shown to improve spatial resolution in reconstructed PET images. However, due to the short half-life of the clinically used isotopes, other long-lived isotopes not used in clinical practice are chosen to perform the PSF measurements, consequently leading to over or under estimation of the true PSF width during reconstruction, due to the difference in positron range. In high resolution brain and preclinical imaging, this effect is of particular importance since the resolution becomes more positron range limited and isotope-specific PSFs can help maximizing the performance benefit from using resolution recovery image reconstruction algorithms. In this work, we use a printing technique to simultaneously measure multiple point sources and demonstrate the feasibility of deriving isotope-dependent system matrices on the High Resolution Research Tomograph (HRRT) by measuring spatially-variant and isotope-specific PSFs using Fluorine-18 and Carbon-11. Initial results based on these 2 isotopes illustrate that even small differences in positron range can result in different PSF maps. The difference is more distinct in the centre of the field of view (FOV) where the full width at half maximum (FWHM) from the positron range has a larger contribution in the overall FWHM compared to the edge of the FOV, where the parallax error dominates the overall FWHM. Further PSF measurements are underway to evaluate clinically used isotopes with larger positron ranges and significantly shorter half-lives. These measurements could be used to create a database of isotope-dependent system matrices to be used within image reconstruction.**

***Index Terms*—PSF, positron range, HRRT, point sources**

I. Introduction

ANALYTICAL calculations and Monte Carlo simulations can be used in PET to estimate the physics-related component of the scanner's system matrix including crystal penetration, intercrystal scattering, photon non-colinearity and positron range in the form of a spatially varying point spread function (PSF). Such methods need to be validated against data emanating from real measurements. Consequently, experimental evaluation of the scanner's spatially variant PSFs is the preferred method for evaluating its spatial resolution characteristics and generating accurate system matrices to be used within resolution recovery image reconstruction algorithms. Such measurements are usually performed using a point source, to sample the PSF at different locations in the FOV. Since only a finite number of locations can be sampled, a parameterization of the system's response is used with the estimated parameters further fitted to smooth functions such as polynomials, to interpolate the parameters in the remaining not sampled positions. Due to the large number of PSF samples needed, long lived isotopes not used in clinical practice, such as Germanium-68 and Sodium-22, are usually the isotopes of choice [1-3]. However this means that the PSF models within the image reconstruction do not correspond to those needed for the data to be reconstructed, either over or under-estimating the PSF width during image reconstruction due to the difference in positron range. In whole-body PET/CT scanners, this effect can only be of importance when the difference in positron range between the isotopes used to measure the PSF and generate the data to be reconstructed, is substantial, as the spatial resolution is dominated by the non-colinearity, crystal size and parallax error with the positron range having little effect on the PSF. However, in high resolution brain or preclinical PET imaging the PSF becomes more isotope-dependent since positron range becomes the limiting resolution degradation factor, thus accentuating the effect of over or under-estimation of the PSF width and signifying the need for isotope-specific PSFs. Measuring the spatially variant isotope-specific PSFs from short-lived isotopes having greater positron ranges is very challenging due to the rapid decay and the multitude of positions needing to be sampled. However, a previously proposed technique based on printing an array of point sources to simultaneously sample the PSF at multiple positions, can facilitate measurements from short-lived isotopes (not previously practical with single source acquisitions based on robotic equipment) [4].

In this work, we apply such a technique to demonstrate the feasibility of measuring isotope-specific system matrices on the HRRT scanner and evaluate the effect of positron range on the spatially-variant PSF.

F. A. Kotasidis is with the Division of Nuclear Medicine and Molecular Imaging, Geneva University Hospital, Geneva Switzerland and Wolfson Molecular Imaging Centre, MAHSC, University of Manchester, Manchester UK

J.C. Matthews, J. Anton-Rodriguez and M. Green are with the Wolfson Molecular Imaging Centre, MAHSC, University of Manchester, Manchester, UK

A.J. Reader is with the Montreal Neurological Institute, McGill University, Montreal, Canada

G. I.Angelis is with the Brain and Mind Institute, University of Sydney, Sydney, Australia

Habib Zaidi is with the Division of Nuclear Medicine, Geneva University Hospital and Geneva Neuroscience Center, Geneva University, Geneva, Switzerland

II. METHODS

Initial measurements were performed using 2 isotopes, Fluorine-18 and Carbon-11, with a half-life of ~110 and ~20 minutes, respectively. The mean positron range for Carbon-11 and Fluorine-18 is 1.266 mm and 0.660 mm, respectively, with a theoretical difference of 0.606 mm between them [5]. Radioactive printing has been used previously to measure the spatial resolution properties of PET scanners and such a technique can provide fast, uniform and reproducible sources of arbitrary 2-dimensional activity distributions [4,6,7]. In this work, an Inkjet printer was used to print an array of 11 × 15 (axially × radially) radioactive point sources, 1 mm in diameter, with a 1.85 cm and 1.95 cm radial and axial sampling distance respectively. Black ink was mixed with ~1 GBq of Fluorine-18 and/or Carbon-11 solution (0.1-0.2 ml) via injection into a modified cartridge. The array was printed once for the Fluorine-18 point sources, while for the Carbon-11 point sources it was re-printed 3 times to boost the activity and counteract the rapid decay and reduced counting statistics compared to Fluorine-18. The same point source production procedures were followed for both isotopes. The array was placed horizontally in the HRRT FOV, using a Perspex phantom to facilitate accurate positioning and provide annihilating material for the positrons, covering almost the entire radial (-12.95..+ 12.95 cm) and axial (-9.75...+ 9.75 cm) FOV. The phantom was made out of 2 Perspex endplates held by 4 Perspex rods, with axial and transverse dimensions equal to the HRRT's bore, ensuring a tight fit during positioning [7]. The point-source array was scanned in list mode format for 60 minutes using Carbon-11 (~65 million prompts) and for 20 minutes using Fluorine-18 (~100 million prompts), followed by a 6 minute transmission scan for attenuation correction. The data were reconstructed using standard HRRT software, including all corrections for erroneous events (OP-OSEM, 10 iterations - 16 subsets) and the reconstructed PSFs were fitted in image space using a Gaussian mixture model of two 3-D Gaussians with axial, radial and tangential mean and standard deviation components for each Gaussian, as well as a weighting parameter controlling the mixing of the 2 distributions [4,6].

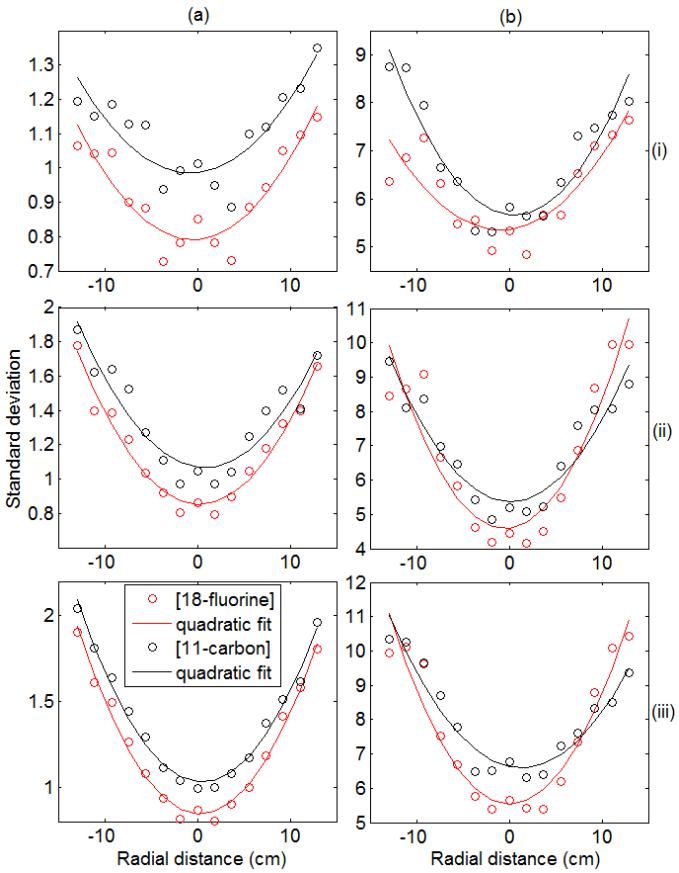

Fig.1. Parameters fitted to functions assuming smooth response transitions to calculate a parametrized response throughout the FOV. Graphs of tangential (i), radial (ii) and axial (iii) standard deviation versus radial distance (axially centred : z=0 cm) for the 1st (a) and 2nd (b) Gaussian and for both isotopes along with the corresponding quadratic fits. Similar fits estimated for every parameter.

III. RESULTS

In total 13 parameters were estimated in image space for each reconstructed PSF. Since parameters were calculated in finite locations throughout the FOV, each parameter was fitted to a quadratic function to describe its variation as a function of radial distance, while assuming axial and rotational translation symmetry [6]. Graphs of the tangential, radial and axial

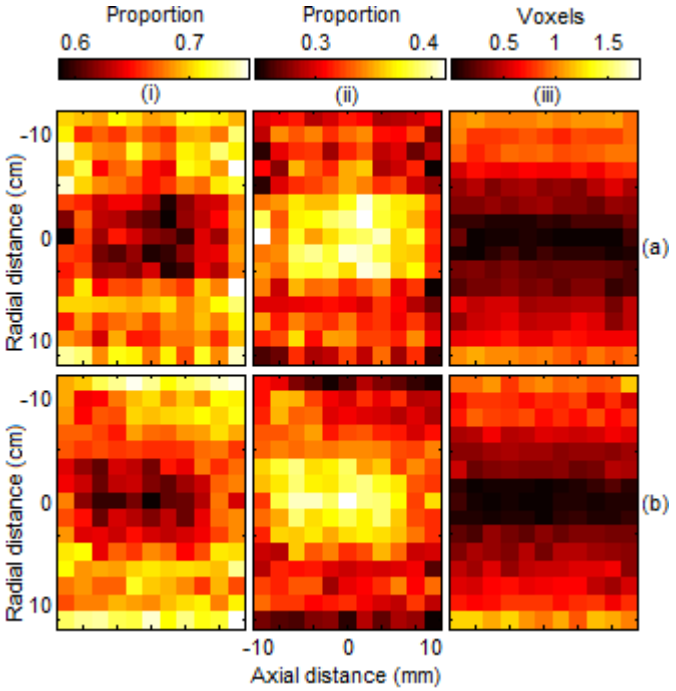

Fig.2. Parametric maps of the proportion coefficient between the 1st (i) and 2nd (ii) Gaussian distribution (sum to 1) for Carbon-11 (a) and Fluorine-18 (b) as well as the respective radial asymmetry for each isotope given as the displacement between the radial means of the 2 Gaussian distributions in voxel units (iii).

standard deviation as a function of radial distance are plotted in Fig. 1 for both Fluorine-18 and Carbon-11 for the 1st (Fig 1(a)) and 2nd (Fig 1(b)) Gaussian distribution, along with the corresponding quadratic fit for each parameter. As the 1st Gaussian accounts for the main distribution, it has a smaller standard deviation compared to the 2nd which accounts for the tails of the PSF and as such it is broader. Looking across the 2 isotopes, Carbon-11 appears to produce an increased standard deviation compared to Fluorine-18 in both Gaussian distributions. The difference is more pronounced towards the centre of the FOV, with the difference in standard deviation between the 2 isotopes being closely matched towards the edge of the radial FOV.

Parametric maps of the mixing proportions between the 2 Gaussians are shown in Fig. 2 (i,ii) both for Carbon-11 (Fig. 2(a)) and Fluorine-18 (Fig. 2(b)) while (Fig. 2(iii)) shows the radial asymmetry given as the difference in the radial means between the 2 Gaussians for the 2 isotopes (a-b). Looking at the mixing proportions, no apparent difference is seen between

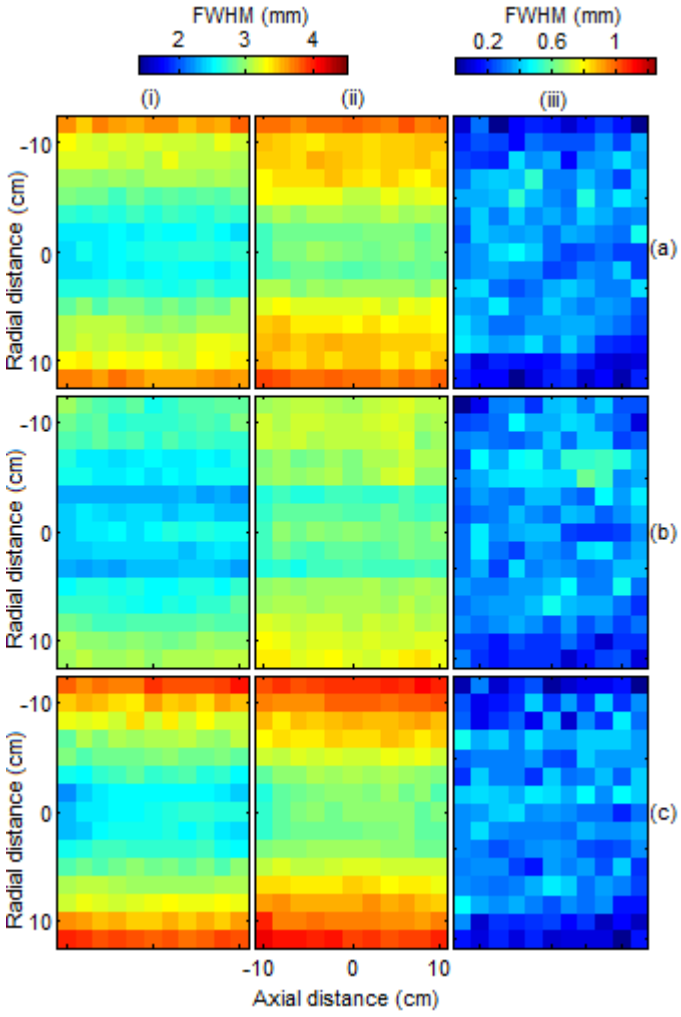

Fig.3. Parametric maps of radial (a), tangential (b) and axial (c) FWHM on the HRRT, as a function of radial and axial distance for Fluorine-18(i), Carbon-11(ii) and their difference (iii).

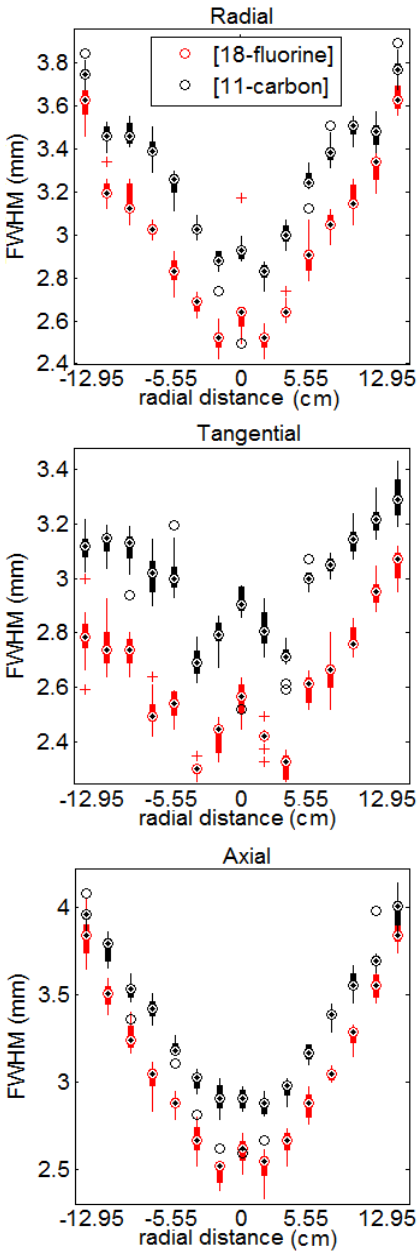

Fig.4. Box-Whisker plots of the radial, tangential and axial FWHM versus radial distance for Carbon-11 and Fluorine-18, where each box represents the axial variation of the FWHM with the top and bottom showing the 25th and 75th percentile.

the 2 isotopes, signifying that going from Fluorine-18 (Fig. 2 (b)) to Carbon-11 (Fig. 2 (a)), the increase in the standard deviation is equally attributed to an increase in the central fast decreasing part of the distribution accounted for by the 1st Gaussian and the slowly decreasing tails accounted for by the 2nd Gaussian. Looking at the radial asymmetry and comparing it across the 2 isotopes no apparent difference is seen. This is to be expected as the asymmetry is caused by the parallax error and as such, it is independent of the positron range.

Parametric maps of FWHM are shown in Fig. 3 for Fluorine-18 (Fig 3(i)) and Carbon-11 (Fig 1(ii)) PSFs. For both isotopes, the axial FWHM is the highest (Fig 3 (c)) followed by the radial and tangential (Fig 1 (a) and Fig 3 (b), respectively). Comparing the PSF between the 2 isotopes, the

Carbon-11 FWHM appears to be noticeably greater both axially, radially and tangentially compared to the ones obtained with Fluorine-18. In the axial FWHM, the resolution increases from 2.59 mm in the centre of the FOV (z=0, r=0) using Fluorine-18 to 2.96 mm using Carbon-11, while at the edge of the radial FOV (z=0, r=12.9cm) it increases from 3.78 mm to 3.92 mm. Similar variations are observed in the radial and tangential FWHM. The difference in FWHM between the 2 isotopes is visualized in Fig. 3 (iii). The axial, radial and tangential FWHM as a function of radial distance is summarized in Fig. 4 for the 2 isotopes, with the box representing the FWHM axial deviation at each radial position and the whiskers showing the 25th and 75th percentile. What is immediately apparent is that the difference is more pronounced in the centre of the radial FOV (also seen in Fig. 1) with differences up to ~0.5mm in the axial, radial and tangential FWHM while at the edge of the radial FOV the differences are minimal (up to ~0.2 mm).

IV. Discussion

A printing technique was used to experimentally calculate isotope-specific system matrices by measuring the spatially variant PSF on the HRRT scanner based on clinically used isotopes. Experimentally measured PSF maps are now used in most modern PET scanners, with such information incorporated within resolution recovery image reconstruction algorithms. Previous methods for deriving such PSF maps, using single source acquisitions, necessitated the use of long-lived, high energy positron-emitting isotopes different from those used in clinical practice. Consequently the true PSF width is over or under-estimated since the overall PSF receives a contribution from the positron range of the isotope used to sample the PSF. This effect is of most importance in high resolution imaging where the positron range becomes the dominating spatial resolution degradation effect. As such using isotope-specific PSFs within spatially variant and isotope specific resolution recovery image reconstruction algorithms can further enhance spatial resolution by realizing the full benefits of PSF modeling.

From the results presented using a high resolution scanner where all the detector related resolution degradation effects account for less on the overall spatial resolution compared to a whole body scanner, even the small difference in positron range between Fluorine-18 and Carbon-11 is sufficient to affect the overall PSF. This effect is less distinct towards the edge of the radial FOV and can be attributed to the fact that parallax error has a significantly larger contribution to the FWHM compared to the centre of the FOV and any increase in the positron range will have a smaller impact on the overall FWHM. Using isotopes with even higher positron range will result in the overall FWHM being dominated by the positron range FWHM, effectively making the spatial resolution invariant throughout the FOV as the parallax error will have a small contribution in the overall resolution. As such going to isotopes with higher positron range, such as Oxygen-15, or Rubidium-82, even a spatially invariant PSF might be sufficient to capture the resolution degrading physics effects, since the spatially variant component of the spatial resolution has a small impact on the overall resolution characteristics of the scanner..

V. Conclusion

Experimentally measured isotope-specific system matrices based on clinically used isotopes can be derived fast and efficiently using a printing technique. Initial results show that in high resolution PET imaging, even a small increase in positron range has a noticeable effect on the measured PSFs due to the relative impact of the positron range on the overall spatial resolution characteristics. Additional measurements can be done to increase the PSF database based on clinically used isotopes by evaluating more energetic isotopes, such as Oxygen-15 and Rubidium-82 where the impact of the larger positron range on the PSF maps is even greater. Isotope-specific PSF kernels can then be used with isotope-specific resolution recovery image reconstruction algorithms in PET to obtain the full benefits of PSF-based reconstruction avoiding under/over-estimating the PSF width.

VI. Reference

[1] V. Y. Panin, F. Kehren, C. Michel, and M. Casey, "Fully 3-D PET reconstruction with system matrix derived from point source measurements.," *IEEE Trans Med Imaging,* vol. 25, pp. 907-921, 2006.

[2] E. Rapisarda, V. Bettinardi, K. Thielemans, and M. C. Gilardi, "Image-based point spread function implementation in a fully 3D OSEM reconstruction algorithm for PET.," *Phys Med Biol,* vol. 55, pp. 4131-4151, Jul 21 2010.

[3] A. M. Alessio, C. W. Stearns, S. Tong, S. G. Ross, S. Kohlmyer, A. Ganin*, et al.*, "Application and evaluation of a measured spatially variant system model for PET image reconstruction.," *IEEE Trans Med Imaging,* vol. 29, pp. 938-949, 2010.

[4] F. A. Kotasidis, J. C. Matthews, G. I. Angelis, P. J. Noonan, A. Jackson, P. Price*, et al.*, "Single scan parameterization of space-variant point spread functions in image space via a printed array: the impact for two PET/CT scanners.," *Phys Med Biol,* vol. 56, pp. 2917-2942, May 21 2011.

[5] W. Lehnert , M. C. Gregoire, A. Reilhac, S. R. Meikle ., "Analytical positron range modelling in heterogeneous media for PET Monte Carlo simulation. .," *Phys Med Biol,* vol. 56, pp. 3313-3335, June 7 2011.

[6] F. A. Kotasidis, G. I. Angelis, J. Henderson, A. Buckley, P. J. Markiewicz, M. Green, M. J. Anton-Rodriguez, W. R. Lionheart, A. J. Reader, J. C. Matthews.," Evaluation of image based spatially variant and count rate dependant point spread functions on the HRRT PET scanner .," IEEE NSS & MIC Conf. Rec, pp 3595 - 3596, 2

[7] P. J. Markiewicz, G. I. Angelis, F. Kotasidis, M. Green, W. R. Lionheart, A. J. Reader*, et al.*, "A custom-built PET phantom design for quantitative imaging of printed distributions.," *Phys Med Biol,* vol. 56, pp. N247-261, Nov 7 2011.